

Unique Role of Oxygen in Regulation of Hepatic Monooxygenation and Glucuronidation

YI-REN WU, FREDERICK C. KAUFFMAN, WEI QU, PATRICIA GANEY, and RONALD G. THURMAN

Laboratory of Hepatobiology and Toxicology, Department of Pharmacology, University of North Carolina at Chapel Hill, Chapel Hill, North Carolina 27599-7365 (Y.W., W.Q., P.G., R.G.T.) and Department of Pharmacology and Toxicology, Rutgers University, Piscataway, New Jersey 08854 (F.C.K.)

Received January 12, 1990; Accepted April 13, 1990

SUMMARY

The purpose of this study was to evaluate the hypothesis that NADPH supply in intact cells is regulated by oxygen tension. This was accomplished by studying monooxygenation in perfused livers from *Ah* locus-responsive C57BL/6J mice, where rates of monooxygenation are high. Elevation of flow rate decreases the hepatic O₂ gradient and increases O₂ delivery to the organ. Under these conditions, rates of *p*-nitroanisole *O*-demethylation were 2–3 times higher in perfused livers from fed or fasted mice at high (10 ml/min) compared with normal (5 ml/min) flow rates. Rates of monooxygenation were directly proportional to oxygen tension (half-maximal rates occurred with approximately 400 μ M O₂). On the other hand, rates were independent of oxygen concentration in isolated microsomes where NADPH was supplied in excess. The decrease in rate due to diminished O₂ concentration in the intact organ could not be attributed to hypoxia, because O₂ tension in the effluent perfusate exceeded 50 μ M even when influent perfusate was saturated with 25% O₂

and ATP/ADP ratios were in the normal range. Thus, monooxygenation of *p*-nitroanisole in perfused mouse liver is dependent on oxygen tension. Similarly, glucuronidation of *p*-nitrophenol was oxygen dependent in the intact organ but not in isolated microsomes supplemented with UDP-glucuronic acid. Taken together, these data support the hypothesis that, at high oxygen tensions (e.g., in periportal regions of the liver lobule), mitochondrial activity is increased, which in turn enhances NADPH and UDP-glucuronic acid turnover, leading to accelerated rates of monooxygenation and glucuronidation in intact cells. In support of this idea, NH₄Cl, which utilizes NADPH for urea synthesis, inhibited monooxygenation in the perfused mouse liver at high but not low flow rates. Thus, important phase I and II detoxification reactions are regulated indirectly by the hepatic oxygen gradient, via mechanisms involving cofactor supply, when cytochrome P-450 is not limiting.

Monooxygenation in the intact cell is influenced by at least two factors in addition to the supply of substrate, the activity of components of the monooxygenase pathway (i.e., cytochrome P-450) and the availability of cellular NADPH (1). The cytochrome P-450 systems are highly active in *Ah* locus-responsive mice (e.g., C57BL), particularly after induction with 3-methylcholanthrene or β -naphthoflavone. Treatment of *Ah* locus-responsive mice with 3-methylcholanthrene has been shown to increase not only the levels of cytochrome P-450 but also the ability of the liver to supply NADPH (2). This latter conclusion is based on the observation that rates of *p*-nitroanisole *O*-demethylation, which decline in livers from untreated mice even when oxygen and substrate were supplied in excess, were sustained at high values for long periods of time in livers from 3-methylcholanthrene-treated *Ah* locus-responsive mice (2).

Recently, Ganey *et al.* (3) demonstrated that the anticancer

drug Adriamycin, which undergoes redox cycling, was toxic only in oxygen-rich periportal regions of the liver lobule in the perfused liver. Redox cycling of drugs with a quinone nucleus requires oxygen and reducing equivalents [e.g., NAD(P)H]. Further, oxygen tension in perfused liver was over 1 order of magnitude higher than levels needed for maximal rates of redox cycling in isolated membranes. Because a direct effect of oxygen could not explain the effect of Adriamycin, the authors suggested that oxygen tension most likely acts by influencing NADPH supply.

On the other hand, measurement of rates of monooxygenation of ethoxycoumarin in periportal and pericentral regions of the liver lobule suggested that both cofactor supply and activity of components of the cytochrome P-450 system participate in regulation of hepatic monooxygenation (4). However, rates of monooxygenation were low (<5 μ mol/g/hr), whereas rates of redox cycling were considerably higher (about 50–60 μ mol/g/hr). Thus, O₂ tension may be limiting for monooxygenation or conjugation when the activity of cytochrome P-450 is high. To test this possibility, monooxygenation was studied in livers

This work was supported in part by grants from the National Institute of Environmental Health Sciences and the National Cancer Institute (ES-02759 and CA-20807).

from *Ah* locus-responsive mice, where rates of monooxygenation are very high (2).

Materials and Methods

Experimental animals. Male C57BL/6J mice (The Jackson Laboratory), age 5–15 weeks, were allowed free access to food and tap water (fed) or were deprived of food for 24–36 hr before liver perfusion (fasted). All mice were injected intraperitoneally once daily with β -naphthoflavone (80 mg/kg) in corn oil (8 mg/ml) for 3 days.

Mouse liver perfusion. The technique of mouse liver perfusion is explained in detail elsewhere (5). Briefly, Krebs-Henseleit bicarbonate buffer (pH 7.4, 37°) was saturated with an oxygen-carbon dioxide mixture (95:5) and pumped into the portal vein at rates of 5 (low flow) or 10 (high flow) ml/min. In some experiments the direction of flow was reversed (retrograde perfusion).

Rates of monooxygenation assessed by *p*-nitrophenol production from *p*-nitroanisole. *p*-Nitroanisole (0.2 mM) was dissolved in Krebs-Henseleit buffer, and *p*-nitrophenolate ion concentration was monitored spectrophotometrically in samples of effluent perfusate collected at 2-min intervals, as described elsewhere (2). Glucuronide and sulfate conjugates of *p*-nitrophenol were measured as free *p*-nitrophenol following enzymatic cleavage, as described previously (6). Under the conditions employed, 80–90% of the conjugates were glucuronides (7). Rates of monooxygenation were determined from the concentration of free and conjugated *p*-nitrophenol formed from *p*-nitroanisole and measured in the effluent perfusate, the flow rate, and the liver wet weight. In a similar manner, conjugation was measured following infusion of *p*-nitrophenol (0.1 mM) instead of *p*-nitroanisole. The effluent perfusate was directed past a Clark-type oxygen electrode before being discarded. Rates of oxygen uptake or metabolite production were calculated from the influent minus effluent concentration differences, the flow rate, and the liver wet weight.

Microsomal monooxygenation and glucuronidation. Hepatic microsomes were prepared by standard techniques of differential centrifugation (8), and *p*-nitroanisole *O*-demethylase activity was determined in microsomal pellets resuspended in 0.15 M KCl. Assays were performed at 37° in 25-ml Erlenmeyer flasks containing 5 mM MgCl₂, 0.7 mM *p*-nitroanisole, microsomes (4–6 mg of protein/ml), and an NADPH-generating system consisting of 0.4 mM NADP⁺, 30 mM isocitrate, and 0.2 units of isocitrate dehydrogenase, in a final volume of 2.0 ml of 0.18 M potassium phosphate buffer, pH 7.4. Incubations were initiated by the addition of the NADPH-generating system and were terminated after 10 or 20 min by the addition of 0.5 ml of 0.6 M perchloric acid. After centrifugation to remove denatured protein, 1.0 ml of supernatant was mixed with 0.1 ml of 12 N NaOH. This mixture was recentrifuged and the supernatant was used for the spectrophotometric determination of *p*-nitrophenol concentration at 436 nm ($\epsilon_{436} = 7.11 \text{ mM}^{-1} \text{ cm}^{-1}$).

Microsomal *p*-nitrophenol glucuronosyltransferase activity was assayed using UDPGA (0.5 mM) as cofactor and *p*-nitrophenol (5 mM) as substrate (7), as described in detail elsewhere. Protein was determined by the biuret reaction (9).

Results

***p*-Nitroanisole metabolism at different flow rates in fed and fasted mouse livers.** As a means of varying the oxygen gradient across the liver lobule, perfusions were performed at both high (10 ml/min) and low (5 ml/min) flow rates in β -naphthoflavone-induced mice. In fed mouse livers perfused at high flow rates, upon infusion of *p*-nitroanisole, total *p*-nitrophenolate production quickly (within 10 min) reached maximal rates of about 25 $\mu\text{mol/g/hr}$. About half of the *p*-nitrophenol formed was free and half was conjugated (Fig. 1A; Table 1). At both flow rates studied, maximal rates were constant until *p*-nitroanisole infusion was terminated; values then

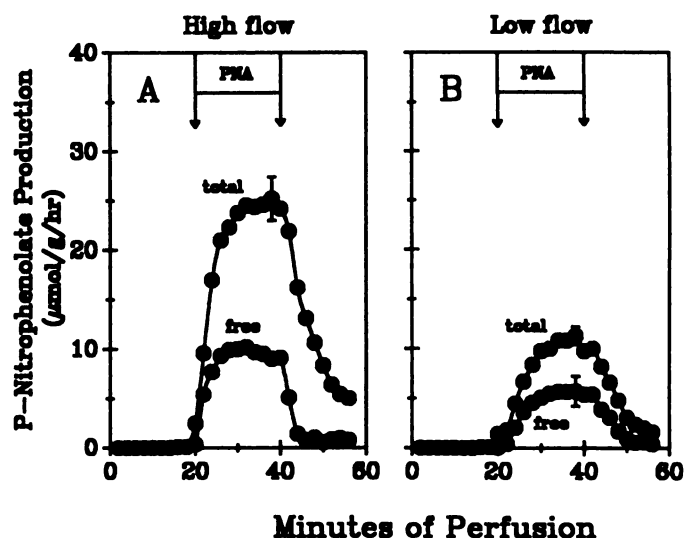


Fig. 1. Effect of perfusate flow rate on *p*-nitroanisole metabolism in perfused livers from fed mice. Livers from fed β -naphthoflavone-treated mice were perfused as described in Materials and Methods at high (A) or low (B) flow rates for 20 min. *p*-Nitroanisole (PNA) (200 μM) was infused for 20 min, as indicated by the arrows and the horizontal bar. Samples of perfusate were collected at 1–2-min intervals and analyzed for total and free *p*-nitrophenol, as described in Materials and Methods. Mean \pm representative standard error of six experiments/group.

declined rapidly to baseline (Fig. 1). At low flow rates, total *p*-nitrophenolate production was maximal at values just above 10 $\mu\text{mol/g/hr}$ and, again, about half was free and half was conjugated (Fig. 1B; Table 1).

Fasting decreases substrate for the generation of NADPH via the pentose cycle. In the fasted state at high flow rate, *p*-nitrophenolate production was also maximal at values around 25 $\mu\text{mol/g/hr}$; however, unlike livers from fed mice, maximal rates were maintained for only 1–2 min and declined steadily by about 30% over 20 subsequent min of perfusion, despite continued perfusion with *p*-nitroanisole (Fig. 2A). This decline was observed in the rates of production of total (free plus conjugated) *p*-nitrophenol as well as free phenol (Fig. 2A; Table 1). Interestingly, this phenomenon was not observed in livers from fasted mice perfused at low flow rates. These rates of production were constant for 20 min at values similar to those observed in livers from fed mice perfused at low flow rates (Fig. 2B; Table 1).

To investigate whether substrate concentration was limiting for this reaction, the effect of higher concentrations (400 μM) of *p*-nitroanisole on *p*-nitrophenolate production was studied. Doubling the substrate concentration did not affect rates of *p*-nitrophenolate production (Table 1). Furthermore, reversing the direction of perfusate flow from anterograde to retrograde also did not affect rates of *p*-nitrophenolate production from *p*-nitroanisole (Table 1). Taken together, these results indicate that substrate supply is not limiting for monooxygenation at either flow rate studied.

Effect of perfusate oxygen concentration on *p*-nitroanisole monooxygenation and glucuronidation in perfused liver. When the perfusate was saturated with 95% oxygen, *p*-nitroanisole was converted into *p*-nitrophenol at maximal rates of about 25 $\mu\text{mol/g/hr}$ in experiments at high flow rates. (Fig. 1A; Table 1). When influent oxygen concentration was decreased, peak rates of monooxygenation were correspondingly lower (Fig. 3, Table 2). In fact, a direct rela-

TABLE 1

Effect of flow rate on rates of monooxygenation and glucuronidation of *p*-nitroanisole in perfused mouse liver

Livers from β -naphthoflavone-treated or control mice that had been fed or fasted before experiments were perfused at the flow rates and *p*-nitroanisole concentrations indicated. Data represent maximal values (mean \pm standard error; $n = 4$ or 5/group).

Treatment	Nutritional state	Direction of perfusion	Flow rate	<i>p</i> -Nitroanisole concentration	<i>p</i> -Nitrophenol production	<i>p</i> -Nitrophenol conjugation
			ml/min	μM	$\mu\text{mol/g/hr}$	$\mu\text{mol/g/hr}$
None	Fed	Anterograde	5	200	6.7 ± 0.7	2.1 ± 0.3
None	Fed	Anterograde	10	200	10.9 ± 0.6	4.5 ± 0.5
β -Naphthoflavone	Fed	Anterograde	5	200	11.3 ± 0.8	5.7 ± 1.1
β -Naphthoflavone	Fed	Anterograde	10	200	25.2 ± 1.9	16.2 ± 0.5
β -Naphthoflavone	Fed	Retrograde	10	200	23.2 ± 6.8	11.6 ± 4.4
β -Naphthoflavone	Fed	Anterograde	5	400	7.7 ± 0.6	3.9 ± 0.8
β -Naphthoflavone	Fed	Anterograde	10	400	20.6 ± 2.3	10.9 ± 1.7
β -Naphthoflavone	Fasted	Anterograde	5	200	11.3 ± 2.4	5.0 ± 1.5
β -Naphthoflavone	Fasted	Anterograde	10	200	22.7 ± 2.4	11.0 ± 2.0

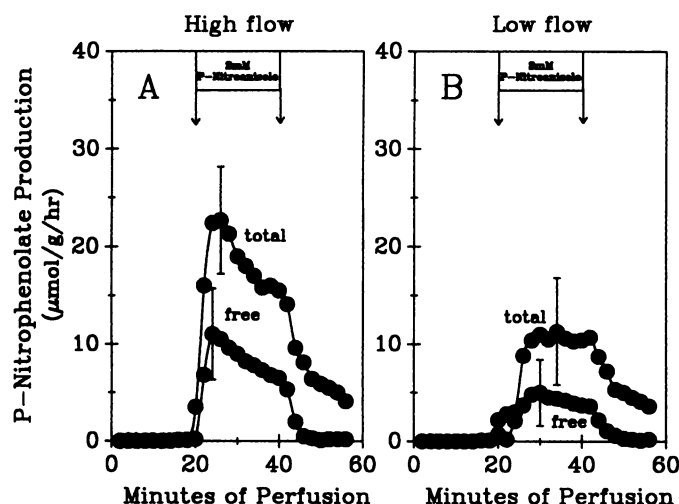


Fig. 2. Effect of perfusate flow rate on *p*-nitroanisole metabolism in perfused livers from fasted β -naphthoflavone-treated mice. Mice were fasted for 24–36 hr before experiments. Other conditions as in Fig. 1.

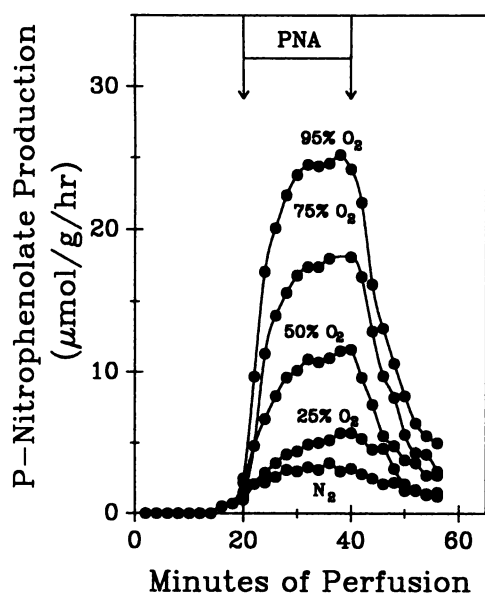


Fig. 3. Effect of oxygen concentration on *p*-nitroanisole metabolism in perfused livers. Livers were perfused with perfusate oxygen concentrations ranging from 0 to 95%, as indicated, at high flow rates. All other conditions as in Fig. 1.

TABLE 2

Effect of perfusate oxygen concentration on rates of oxygen uptake, monooxygenation, and glucuronidation in perfused mouse liver

Livers were perfused with *p*-nitroanisole (200 μM) and with varying influent oxygen concentrations. The oxygen concentration was varied by mixing 95% O_2 /5% CO_2 with 95% N_2 /5% CO_2 to produce the desired oxygen saturation. Values were verified with an oxygen electrode. Maximal rates of *p*-nitrophenol production and conjugation were calculated as described in Materials and Methods. Data represent mean \pm standard error ($n = 4$ or 5).

Influent oxygen saturation	Effluent oxygen concentration	Oxygen uptake	<i>p</i> -Nitrophenol production	<i>p</i> -Nitrophenol conjugation
%	μM	$\mu\text{mol/g/hr}$	$\mu\text{mol/g/hr}$	$\mu\text{mol/g/hr}$
95	814	348 ± 40	25.2 ± 4.4	16.2 ± 5.5
75	643	416 ± 38	19.9 ± 4.8	13.9 ± 5.1
50	429	294 ± 13	11.6 ± 2.4	7.7 ± 1.6
25	214	114 ± 10	5.7 ± 1.1	4.2 ± 1.0
0	0		3.6 ± 0.6	1.5 ± 0.3

tionship ($r = 0.98$) between influent O_2 concentration and maximal rate of monooxygenation was observed.

To measure rates of conjugation at varying oxygen concentrations in the perfused liver, *p*-nitrophenol was infused in the same manner as *p*-nitroanisole. Because 80–90% of the conjugates produced were glucuronides, glucuronidation was monitored by spectrophotometric analysis of effluent perfusate for *p*-nitrophenol following enzymatic hydrolysis with β -glucuronidase. Following 20 min of perfusion with *p*-nitrophenol at five different oxygen concentrations, livers were perfused for 20 min with nitrogen-saturated buffer (Fig. 4, Table 2). As with monooxygenation, rates of glucuronidation were proportional to influent oxygen concentrations (i.e., the change in steady state levels of conjugates formed was proportional to oxygen tension). Maximal rates of glucuronidation were about 16 $\mu\text{mol/g/hr}$ with 95% oxygen and were around 4 $\mu\text{mol/g/hr}$ at 25% oxygen. At all oxygen concentrations studied, rates decreased when oxygen supply was terminated and the changes were largest in livers that had been previously perfused with buffer containing the highest influent oxygen concentrations. Thus, glucuronidation was also oxygen dependent in the perfused liver.

One possible explanation for these results is that oxygen caused limitation of cytochrome P-450 and limited UDPGA synthesis in peripheral regions of the liver lobule due to local hypoxia. This idea was evaluated by examining the oxygen gradient across the liver lobule at various influent oxygen concentrations in β -naphthoflavone-treated C57BL mice. At 95,

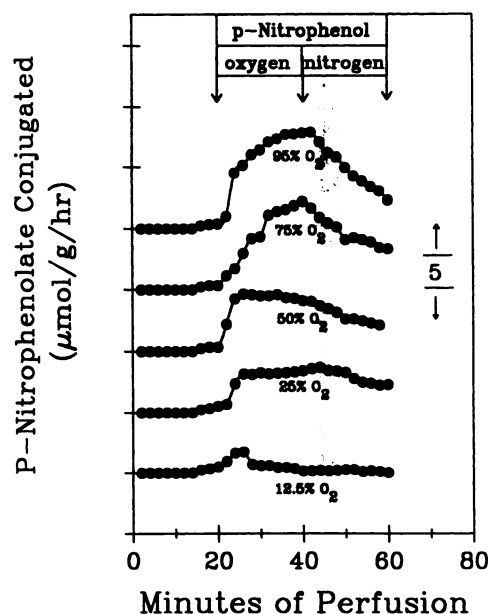


Fig. 4. Effect of oxygen concentration on conjugation of *p*-nitrophenol in the perfused liver. Conditions as in Fig. 3, except that *p*-nitrophenol (0.1 mM) was added instead of *p*-nitroanisole at 20 min, as indicated by arrows and horizontal bars. Perfusate oxygen supply was decreased to zero (nitrogen saturated) at 40 min of perfusion. The area between the two arrows on the right represents 5 μ mol glucuronide produced/g/hr.

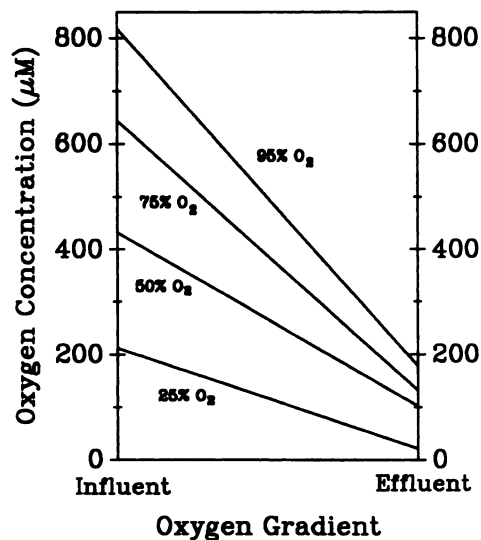


Fig. 5. Oxygen gradient of the perfused liver. Conditions as in Fig. 3. Influent and effluent O₂ concentrations were measured with a Clark-type O₂ electrode, and O₂ gradients were constructed.

75, and 50% influent oxygen concentrations, effluent oxygen concentrations were consistently between 100 and 200 μ M, and only at 25% influent oxygen did the effluent concentration decline to values around 50 μ M oxygen (Fig. 5). Hypoxia was ruled out because ATP/ADP ratios were in the normal range (see Discussion).

Rates of *p*-nitroanisole metabolism at varying oxygen concentrations in microsomes. To test the hypothesis that oxygen regulates *p*-nitroanisole metabolism through control over cofactor supply, *O*-demethylation of *p*-nitroanisole and glucuronidation of *p*-nitrophenol were examined in isolated hepatic microsomes incubated with an NADPH- or UDPGA-generating system, respectively. As expected, both monooxy-

genation (*p*-nitrophenol produced: 95% O₂, 43 \pm 4; 0% O₂, 38 \pm 1 μ mol/g/hr) and conjugation (*p*-nitrophenol conjugated: 181 \pm 11 at 95% O₂, 156 \pm 10 μ mol/g/hr at 0% O₂) were essentially independent of oxygen concentration in microsomes (Fig. 6). This result contrasts sharply with results from perfused liver, where rates of monooxygenation and conjugation were directly proportional to influent oxygen concentrations.

Effect of ammonium chloride on monooxygenation. To test the hypothesis that oxygen controls the supply of NADPH and, thus, regulates the rate of *p*-nitroanisole metabolism, a competitor for NADPH supply was studied. Ammonium chloride is converted into urea and consumes mitochondrial NADPH at high rates in the process. When ammonium chloride was infused, *p*-nitrophenolate production declined sharply by about 30% when perfusions were at high flow rates (Fig. 7A). However, at low flow rates, *p*-nitrophenolate production was unaffected by ammonium chloride (Fig. 7B).

Discussion

Effect of oxygen on monooxygenation in perfused mouse liver. This study was designed to test the hypothesis that oxygen regulates rates of monooxygenation and glucuronidation via cofactor supply. Early work in perfused rat liver suggested that oxygen had little to do with rates of drug metabolism. First, the *K_m* of cytochrome oxidase for oxygen is very low (less than 1 μ M), and one would predict that oxygen is never limiting for monooxygenation under physiological conditions (10). Second, studies using microfiber optics to determine rates of monooxygenation in different regions of the liver lobule of the rat where cytochrome P-450 activity was low suggested that oxygen tension plays an insignificant role in monooxygenation. For example, average oxygen tension is about 2-fold higher in periportal than pericentral regions of the

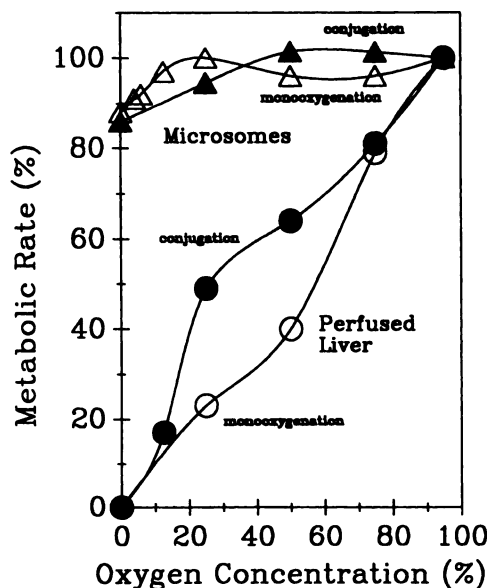


Fig. 6. Rates of *p*-nitroanisole metabolism and *p*-nitrophenol conjugation in isolated microsomes and in the perfused liver at varying oxygen concentrations. Livers were perfused as in Figs. 3 and 4. Hepatic microsomes were prepared and incubated with NADPH (monooxygenation) or UDPGA (conjugation), as described in Materials and Methods. Rates of metabolism are represented as percentage of maximal rates observed with 95% oxygen. Open symbols, rates of monooxygenation; closed symbols, rates of conjugation.

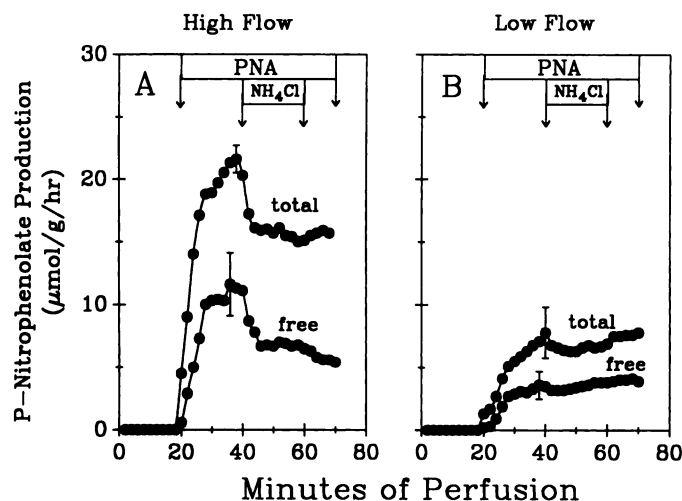


Fig. 7. Effect of ammonium chloride on *p*-nitroanisole metabolism in livers perfused at high and low flow rates. *p*-Nitroanisole (PNA) was infused for 50 min and ammonium chloride (4 mM) was infused for 20 min, as indicated by horizontal bars and arrows. Other conditions as in Fig. 1.

liver lobule. However, ethoxycoumarin *O*-deethylation occurred about twice as fast in pericentral, compared with periportal, areas (4) where cytochrome P-450 predominates (11). On the other hand, levels of cytochrome P-450 were not the only rate-determining factor, because rates in both regions were doubled by infusion of a substrate for NADPH synthesis, xylitol. Rates of monooxygenation in the rat are, however, very low ($<5 \mu\text{mol/g/hr}$). More recently, Ganey *et al.* (3) demonstrated that Adriamycin, a redox cycling quinone-containing anticancer drug, was toxic only in oxygen-rich periportal regions of the liver lobule, and at high oxygen tension in the heart (12). These authors suggested that oxygen may act via production of reducing equivalents.

To test the hypothesis that O_2 tension regulates NADPH supply, a model was selected in which a reaction dependent on NADPH (e.g., monooxygenation of *p*-nitroanisole) could be studied without limitation by cytochrome P-450. This goal was achieved by using *Ah* locus-responsive mice, which display very high rates of monooxygenation, particularly when treated with β -naphthoflavone.

Several experiments were performed to establish whether *p*-nitroanisole *O*-demethylation was oxygen dependent in the perfused liver. Using high and low flow rates as a crude means of altering the oxygen gradient, rates of *p*-nitrophenolate production from *p*-nitroanisole were determined (Fig. 1; Table 1). In each case the higher flow rate produced significantly greater activity of the monooxygenase pathway. To rule out the possibility that this phenomenon arose from an alternate effect of flow rate other than changes in the oxygen gradient, the perfusate oxygen concentration was varied at constant flow rate (Fig. 3). This experiment produced a clear linear relationship between oxygen concentration and peak rate of *p*-nitroanisole monooxygenation in the perfused liver but not in isolated microsomes (Fig. 6). Thus, this interesting effect of oxygen on rates of monooxygenation is only observed in intact cells. One possible explanation for the oxygen dependence of monooxygenation in the perfused liver is that, as the inflow O_2 tension is lowered, a fraction of the liver becomes hypoxic. However, as the O_2 tension is lowered, energy demands also decline (Fig. 5) (16). Only when influent O_2 tensions were at 25% could

hypoxia contribute to diminished rates of monooxygenation. This conclusion was supported by the observation that the ATP/ADP ratio, which decreases dramatically during hypoxia (13), was unaffected by decreasing inflow O_2 tension in these experiments (95% O_2 , 4.0 ± 0.4 ; 75% O_2 , 4.5 ± 0.9 ; 50% O_2 , 4.0 ± 0.8 ; $n = 4$ or 5/group).

Role of NADPH supply. These results led us to consider the possibility that oxygen acts via cofactor supply. As mentioned above, rates of monooxygenation studied in isolated microsomes supplied with excess NADPH were independent of O_2 tension. Thus, the effect of oxygen was abolished when the incubation was supplemented with excess NADPH. Therefore, it seems plausible to propose that oxygen regulates monooxygenation by control over cofactor supply. Changes in the kinetics of *p*-nitroanisole *O*-demethylation at high but not at low flow rates support this idea. Previously, we observed that rates of *p*-nitroanisole *O*-demethylation declined over time, despite adequate oxygen and substrate supply (2, 14). Because monooxygenation requires only substrate, oxygen, and NADPH, it was concluded that NADPH supply is rate limiting.

The hypothesis that O_2 operates via cofactor supply was also supported by introduction of a competitor for NADPH supply at high and low O_2 tensions. Ammonium chloride, which is converted into urea and uses mitochondrial NADPH (15), caused a significant decrease in monooxygenation at high flow rates. At low flow rates, the decline in monooxygenation caused by NH_4Cl was negligible, indicating that cofactor supply was not limiting when O_2 delivery was diminished. Taken together, these data strongly support the hypothesis that oxygen influences monooxygenation via NADPH supply.

Relationship between oxygen tension and metabolic activity. Several years ago, Matsumura and Thurman (16) developed a method employing miniature O_2 electrodes to measure rates of O_2 uptake in periportal and pericentral regions of the liver lobule. In those and subsequent studies (17), O_2 uptake was consistently 2- to 3-fold higher in periportal than pericentral regions of the liver lobule. Moreover, when the direction of perfusion was reversed, O_2 uptake predominated in pericentral regions. Thus, O_2 uptake followed the O_2 gradient (i.e., the local O_2 tension), irrespective of the direction of flow. Subsequently, a number of studies have demonstrated that synthesis of glucose (18) and urea (17), as well as sensitivity to hepatotoxins such as allyl alcohol (19), menadione (20), and ethylhexanol (21), follow the O_2 gradient in the liver. The mechanism for this phenomenon is not clear but most likely involves an oxygen sensor, perhaps an enzyme with a high K_m for oxygen, that produces signal molecules. Active mitochondria make more ATP, and this could drive NADPH synthesis via the transhydrogenase reaction. This is the most likely explanation for the mechanism by which oxygen regulates NADPH supply and, consequently, monooxygenation.

Oxygen dependence of glucuronidation. The *p*-nitrophenolate glucuronidation reaction proved to be similarly oxygen dependent in the perfused liver (Fig. 4). Because the cofactor for glucuronidation, UDPGA, abolished the dependence on oxygen when it was added to isolated microsomes, we conclude here as well that O_2 dependence is observed only in the whole cell. As mentioned above, turnover of ATP is O_2 dependent. Because UDPGA synthesis requires ATP, the effect of O_2 on glucuronidation is also most likely due to its action on cofactor (UDPGA) synthesis.

Thus, these studies demonstrate that, after exposure of a genetically susceptible strain of mice to a carcinogen, regulation of monooxygenation and glucuronidation is altered dramatically. Under these conditions, cofactor supply for high rates of monooxygenation and glucuronidation is regulated indirectly by oxygen.

References

1. Thurman, R. G., and F. C. Kauffman. Factors regulating drug metabolism in intact hepatocytes. *Pharmacol. Rev.* 31:229-251 (1980).
2. Conway, J. G., F. C. Kauffman, and R. G. Thurman. Genetic regulation of NADPH supply in perfused mouse liver: role of the *Ah* locus during induction by 3-methylcholanthrene. *J. Biol. Chem.* 258:3825-3831 (1983).
3. Ganey, P. E., F. C. Kauffman, and R. G. Thurman. Regulation of oxygen-dependent hepatotoxicity due to doxorubicin: role of reducing equivalent supply in perfused rat liver. *Mol. Pharmacol.* 34:695-701 (1988).
4. Belinsky, S. A., F. C. Kauffman, S. Ji, J. J. Lemasters, and R. G. Thurman. Stimulation of mixed-function oxidation of 7-ethoxycoumarin in periportal and pericentral regions of the perfused rat liver by xylitol. *Eur. J. Biochem.* 137:1-6 (1983).
5. Scholz, R., W. Hansen, and R. G. Thurman. Interaction of mixed-function oxidation with biosynthetic processes. I. Inhibition of gluconeogenesis by aminopyrine in perfused rat liver. *Eur. J. Biochem.* 38:64-72 (1973).
6. Reinke, L. A., F. C. Kauffman, and R. G. Thurman. Stimulation of *p*-nitroanisole *O*-demethylation by ethanol in perfused livers from fasted rats. *J. Pharmacol. Exp. Ther.* 211:133-139 (1979).
7. Reinke, L. A., S. A. Belinsky, R. K. Evans, F. C. Kauffman, and R. G. Thurman. Conjugation of *p*-nitrophenol in the perfused rat liver: the effect of substrate concentration and carbohydrate reserves. *J. Pharmacol. Exp. Ther.* 217:863-870 (1981).
8. Remmer, H., J. Schenkman, R. W. Estabrook, H. Sasame, J. Gillette, S. Narashimulu, D. Y. Cooper, and O. Rosenthal. Drug interaction with hepatic microsomal cytochrome. *Mol. Pharmacol.* 2:187-190 (1966).
9. Gornall, A. G., C. J. Bardawill, and M. M. David. Determination of serum proteins by means of the biuret reaction. *J. Biol. Chem.* 177:751-766 (1949).
10. Cooper, D. Y., S. Narashimulu, O. Rosenthal, and R. W. Estabrook. Spectral and kinetic studies of microsomal pigments, in *Oxidases and Related Redox Systems* (T. E. King, H. S. Mason, and M. Morrison, eds.). Wiley, New York, 838-855 (1966).
11. Baron, J., T. T. Kawabata, S. A. Knapp, J. M. Voight, J. A. Reddick, W. B. Jakoby, and F. P. Guengerich. Intrahepatic distribution of xenobiotic-metabolizing enzymes, in *Foreign Compound Metabolism* (J. Caldwell and G. D. Paulson, eds.). Taylor and Francis, London, 17-36 (1984).
12. Morgan, B. P. Mechanisms of tissue damage by the membrane attack complex of complement. *Complement Inflamm.* 6:104-111 (1989).
13. Anundi, I., J. King, D. A. Owen, H. Schneider, J. J. Lemasters, and R. G. Thurman. Fructose prevents hypoxic cell death in liver. *Am. J. Physiol.* 253:G390-G396 (1987).
14. Thurman, R. G., D. P. Marazzo, L. S. Jones, and F. C. Kauffman. The continuous kinetic determination of *p*-nitroanisole *O*-demethylation in hemoglobin-free perfused rat liver. *J. Pharmacol. Exp. Ther.* 201:498-506 (1977).
15. Sies, H., T. P. M. Akerboom, and J. M. Tager. Mitochondrial and cytosolic NADPH systems and isocitrate dehydrogenase indicator metabolites during ureogenesis from ammonia in isolated rat hepatocytes. *Eur. J. Biochem.* 72:301-307 (1977).
16. Matsumura, T., and R. G. Thurman. Measuring rates of O₂ uptake in periportal and pericentral regions of liver lobule: stop-flow experiments with perfused liver. *Am. J. Physiol.* 244:G656-G659 (1983).
17. Kari, F. W., H. Yoshihara, and R. G. Thurman. Urea synthesis from ammonia in periportal and pericentral regions of the liver lobule: effect of oxygen. *Eur. J. Biochem.* 163:1-7 (1987).
18. Matsumura, T., T. Kashiwagi, H. Meren, and R. G. Thurman. Gluconeogenesis predominates in periportal regions of the liver lobule. *Eur. J. Biochem.* 144:409-415 (1984).
19. Badr, M. Z., S. A. Belinsky, F. C. Kauffman, and R. G. Thurman. Mechanism of hepatotoxicity to periportal regions of the liver lobule due to allyl alcohol: role of oxygen and lipid peroxidation. *J. Pharmacol. Exp. Ther.* 238:1138-1142 (1986).
20. Badr, M. Z., H. Yoshihara, F. C. Kauffman, and R. G. Thurman. Menadione causes selective toxicity to periportal regions of the liver lobule. *Toxicol. Lett.* 35:241-246 (1987).
21. Sosenko, I. R. S., S. M. Innis, and L. Frank. Menhaden fish oil, *n* - 3 polyunsaturated fatty acids, and protection of newborn rats from oxygen toxicity. *Pediatr. Res.* 25:399-404 (1989).

Send reprint requests to: Dr. Ronald G. Thurman, Laboratory of Hepatobiology and Toxicology, Department of Pharmacology, University of North Carolina, Chapel Hill, NC 27599-7365.
